A method for studying the stability and the existence of discrete breathers in a chain of coupled symplectic maps

Vassilis Koukouloyannis, Thomas Tziotzios and George Voyatzis
School of Physics, Theoretical Mechanics
Aristotle University of Thessaloniki
54124 Thessaloniki Greece

An one-dimensional chain of weakly coupled symplectic maps is studied. We examine the existence and the size of the stability regions around specific periodic orbits in the phase space of the system with respect to the length of the chain and the coupling strength between the oscillators. In order to accomplish this, we consider a set of orbits defined by a grid of initial conditions in a proper section of the phase space of the system and classify them according to their regularity using the fast Lyapunov indicator (FLI) as a chaos indicator. The correlation between the existence of stability islands and the linear stability of the corresponding periodic orbits is demonstrated. The results of our study are used in order to examine the stability properties of Discrete Breathers (DBs) i.e. spatially localized oscillations in extended systems. Finally, we illustrate how this method can be used in order to indicate the existence of DBs and other breather-like motions.

I. INTRODUCTION

The research topic of discrete breathers has received a great amount of interest in the last two decades since the first indication of their existence by Takeno et al. [1] and the first proof by MacKay and Aubry [2]. By the term Discrete Breather (DB) we denote a spatially-localized and time-periodic motion in a spatially periodic and extended (virtually infinite) system. Usually such a system is a one dimensional chain or a lattice of higher dimension of weakly coupled identical oscillators. By the term localized we refer to a state of the system in which the energy is mainly concentrated around one site of the chain or the lattice, which is called the "central" oscillator. The other sites also oscillate but the amplitude of the oscillation decays, usually exponentially, as we move away from the central oscillator. For more information the reader may refer e.g. to [3–5]

The system under consideration is a system of discrete time, so, we consider an one-dimensional chain of k oscillators, where each individual oscillator is described by a two-dimensional area preserving (symplectic) mapping. In this system a DB is represented by an isolated periodic orbit in the $2k$-dimensional phase space of the system. In [6, 7] this problem has been address using the notion of the continuation from the *anticontinuous limit* $\varepsilon = 0$, where ε denotes the value of the coupling parameter. In this limit, if we consider one "central" oscillator moving in a periodic orbit and all the other oscillators being at rest, a *non-isolated* periodic orbit is defined, which is trivially localized in space and lies in a 1D resonant circle in the phase space of the full system. Each point of this circle corresponds to a periodic orbit with the same property of space localization. Some of these periodic orbits will be continued to provide a DB for $\varepsilon \neq 0$. An analytical formula is provided in [6] in order to calculate the initial conditions of these orbits. So, by taking these initial conditions as starting point, we can calculate numerically the initial conditions for the whole family of the periodic orbits, which correspond to DBs, for increasing ε. But the calculations evolved in the previously mentioned formula are often very complicated or even unfeasible.

In the present work, we attack the problem of calculating initial conditions of DBs using a different approach. We will not use at all the anticontinuous limit but we will consider $\varepsilon \neq 0$ instead. We define a section of the phase space of the system by fixing initial conditions for all the non-central oscillators and we take a grid of initial conditions for the central oscillator in this section. Then we can construct a map by classifying the above defined orbits as *regular* or *chaotic* using a suitable chaos indicator (the *Fast Lyapunov Indicator* or *FLI* in our case). Although the system is high dimensional, in a DB solution the major portion of the energy is concentrated in the mapping which represents the central oscillator. So, the result of this method is expected to be similar to a 2D phase portrait. Consequently, there will be stability regions around the stable isolated periodic orbits which correspond to DBs. This fact will be used in order to locate the DBs. In addition, the existence and size of these stability islands provide us with important information about the stability properties of the specific solutions.

In section 2 we introduce the system of coupled oscillators and the tools used in our study. In section 3 we perform our stability analysis and present our results about the existence and stability of breathers as the length of the chain increases. In section 4 we examine the use of the stability maps in order to calculate initial conditions for various Discrete Breathers or other breather-like motions.

II. MODEL AND TOOLS

Our system is formed by using coupled Suris mappings. The stability of the periodic orbits of the system is studied using linear analysis. The nonlinear stability is established by using FLI stability maps.

A. The model of coupled Suris mappings

The $\mathbb{R}^2 \to \mathbb{R}^2$ *symplectic*, *Suris* mapping is defined as [8]:

$$\begin{aligned} x' &= x + 4\pi^2 y' \qquad \mod 2\pi \\ y' &= y + V'(x) \end{aligned} \tag{1}$$

with

$$V'(x,\delta) = -\frac{1}{\pi^2}\arctan\left(\frac{\delta\sin(x)}{1+\delta\cos(x)}\right), \tag{2}$$

where $0 < \delta < 1$ is a constant, which, in the present work, we select to be $\delta = \frac{1}{3}$. Note that this mappping is *integrable*, i.e it possesses a function $\Phi(x,y)$ which is constant along the orbit

$$\Phi(x',y') = \Phi(x,y) = \cos(2\pi^2 y) + \delta\cos(x - 2\pi^2 y). \tag{3}$$

To the best of our knowledge, the Suris mapping is the only integrable symplectic mapping which possesses a homoclinic loop that separates vibrational and rotational motion. The above features makes the Suris map the most general map to study.

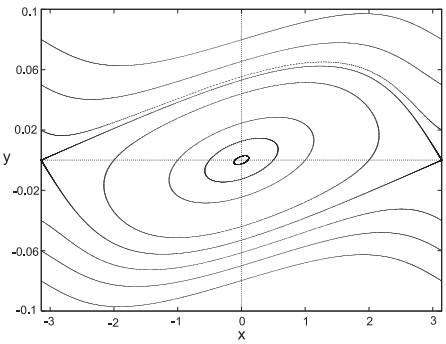

FIG. 1: The integrable Suris map

Consider now that the motion of an oscillator is described by a Suris mapping. Then, a chain of coupled oscillators can be described by a system of symplectic mappings with an appropriate sinusoidal weak nearest-neighbour coupling which preserves the symplectic property of the overall system. Particularly the system is written in the form

$$\begin{aligned} x_i' &= x_i + 4\pi^2 y_i' \qquad \mod 2\pi \\ y_i' &= y_i + V'(x_i) + \varepsilon\sin(x_{i+1} - x_i) + \varepsilon\sin(x_{i-1} - x_i) \end{aligned} \tag{4}$$

where i denotes the i-th oscillator in a chain of length k and ε stands for the strength of the coupling.

In our study we always use an odd number of oscillators considering the ones at the edges of the chain fixed at $(x,y) = (0,0)$. Thus in (4) it is $1 < i < k$ and the oscillator with $i = (k+1)/2$ is the central oscillator. In this sense the chain is symmetric with respect to the central oscillator and the system is of $2(k-2)$ dimensions.

B. Linear stability of periodic orbits

As it is mentioned in the introduction, DBs are associated with periodic solutions of system (4). After the calculation of the initial conditions of a particular periodic orbit, with the method that will be described later, we can examine its linear stability. This is done through the eigenvalues λ_i of the matrix L of the tangent map of (4) calculated for the specific periodic orbit [9]. Since the system is symplectic for every eigenvalue λ_i of L, there is also its reciprocal λ_i^{-1}, its complex conjugate λ^* and of course its reciprocal of the complex conjugate λ_i^{*-1}. So, the eigenvalues of L always appear in what is called a *complex quadruple*. In a linearly stable periodic orbit all the corresponding eigenvalues lie on the unit circle. In this case the eigenvalues appear in pairs since $\lambda^{-1} = \lambda^*$. When the coupling parameter ε of the system increases the eigenvalues λ_i move along the unit circle. When a pair of eigenvalues (λ_i, λ_i^{-1}), collide in $+1$ or -1, they can leave the unit circle and move along the real axis such that $\lambda_i\lambda_i^{-1} \neq \pm 1$. This is called real instability. The second case is when eigenvalues of different pairs collide in the unit circle far from ± 1. Then, if they are of a different Krein kind [10, 11], they can leave the unit circle forming a complex quadruple. This case corresponds to *complex instability*.

C. The fast Lyapunov indicator (FLI) and stability maps

The most common way to check for the chaoticity of a given orbit is the calculation of the maximum Lyapunov exponent or Lyapunov characteristic number (LCN). However it is claimed that the numerical computation of LCN is a rather slow procedure. In order to accelerate this procedure, various *chaoticity indices* have been developed, like FLI (Fast Lyapunov Indicator) [12, 13], SALI (Smaller Alignment Index) [14], RLI (Relative Lyapunov indicator) [15] etc. In the present work we consider the FLI for classifying the system's oscillations as ordered or chaotic. FLI can be defined in the following way :

$$FLI(t) = \sup\left(\log\frac{\|\vec{\xi(t)}\|}{\|\vec{\xi_0}\|}\right) \tag{5}$$

where $\vec{\xi_0}$ is the initial deviation vector in the initial conditions of a particular orbit and $\vec{\xi(t)}$ is the deviation vector after time t. FLI increase linearly in time when the orbit is regular while a super-exponential increase is obtained when the orbit is chaotic. For a discrete system, as (1) or (4), t is substituted by the number n of iterations. An typical example of the evolution of the FLI for a regular and a chaotic orbit is shown in fig.2.

On the $x-y$ plane which correspond to the central oscillator of the system we define a grid of initial conditions.

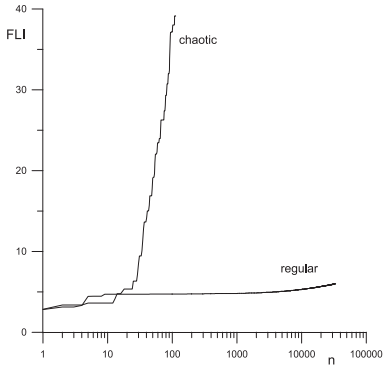

FIG. 2: The evolution of FLI vs the number n of iterations for a chaotic and a regular orbit of the Suris map.

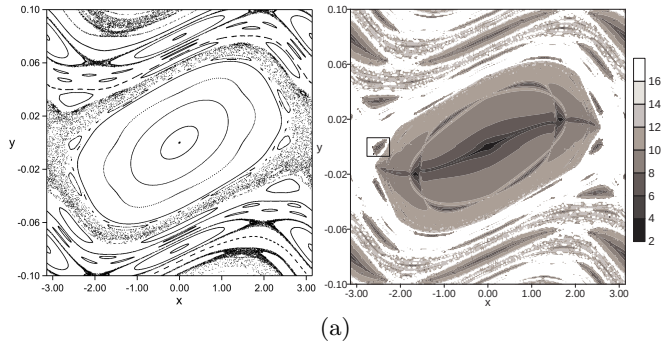

FIG. 3: The system of $k = 3$ oscillators and $\varepsilon = 0.0028$ (a) the phase space of the system and (b) the stability map where white and gray color points correspond to chaotic and regular orbits, respectively.

The initial conditions of the rest oscillators are set to stable equilibrium point (0,0) or are fixed to some particular values. For each initial condition (x, y) we compute the corresponding FLI and a map is formed according to FLI values which are represented by using a color scale. Particularly we consider grids of size 150×150 and for each orbit we compute the FLI value after 5000 iterations. If FLI exceeds the value of 40 we stop the iterations and the orbit is classified as chaotic. Generally, for regular orbits the FLI takes values smaller than 10. Thus, gray regions in the stability maps indicate regular orbits while light regions indicate chaos.

III. STABILITY ANALYSIS

At first we consider a chain consisting only of 3 oscillators in order to test our scan method and compare the results with the linear stability analysis. After that, we increase the length k of the chain in order to examine the effect of the size of the system to the stability properties of the periodic orbits under consideration. We reach the size of $k = 31$ oscillators, where the side effects can be considered as negligible and we can check the existence and stability of Discrete Breathers (DBs).

A. Chain consisting of $k = 3$ oscillators

Apart from the central oscillator, the other two oscillators at the edges of the chain are fixed at $(x, y) = (0, 0)$. Therefore we have only one degree of freedom and the system is given as a 2D perturbed Suris map. In Fig.3a we present the phase space of the system for the perturbation or coupling parameter value $\varepsilon = 0.0028$. We can observe the chaotic layer around the separatrix which divides the phase space into the regions of librational and rotational motion. In both these regions we can distinguish some invariant curves, some chaotic regions and several Poincaré - Birkhoff chains in the center of which stable periodic orbits exist. Beside the phase space, the corresponding stability map is presented too (Fig.3b). We can easily observe the correspondence between the two figures. In particular we shall consider the stability islands around periodic orbits. In the center of the islands periodic orbits exist whose initial conditions can be numerically computed with high accuracy using the Newton-Raphson root finding method, by considering initial estimation inside these islands.

We shall consider the stability chain which correspond to the period-8 orbit. This chain can be found just outside the central stable region of librations and one of its islands is indicated by the square in fig.3b. The stability maps presented in the panels of Fig.4 correspond to a magnification around the specific island of the period-8 orbit. By increasing the value of the parameter ε the size of the island shrinks. In the stability map which corresponds to $\varepsilon = 0.0053$ we can observe the creation of second order islands around the main island. For $\varepsilon = 0.00535$ the island breaks. The bifurcation that occurs is a tangent bifurcation, since the orbit under consideration becomes unstable and two new period-8 orbits are generated.

The results of the linear stability analysis is shown in fig.(5). The value of ε for which the eigenvalues of the periodic orbit leave the unit circle at unity and instability is formed is $\varepsilon_{cr} \simeq 0.0053$, which is in close agreement to the results obtained by the stability maps.

B. Chain consisting of $k = 5$ oscillators

As before the oscillators at the edges of the chain are fixed at the equilibrium $(x, y) = (0, 0)$ and the system is of three degrees of freedom or six-dimensional. Using the calculated initial conditions for the period-8 orbit in the $k = 3$ case and putting the rest oscillators at rest as initial estimation, we calculate the period-8 orbit for the $k = 5$ case and for a given value of ε. We fix the non-central oscillators in these calculated initial conditions

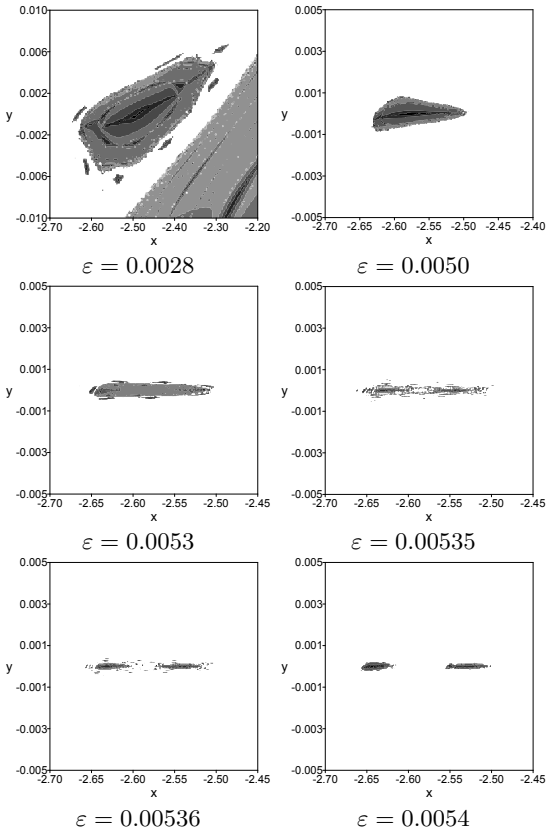

FIG. 4: The evolution of a period-8 stability island in a $k = 3$ chain for increasing values of ε.

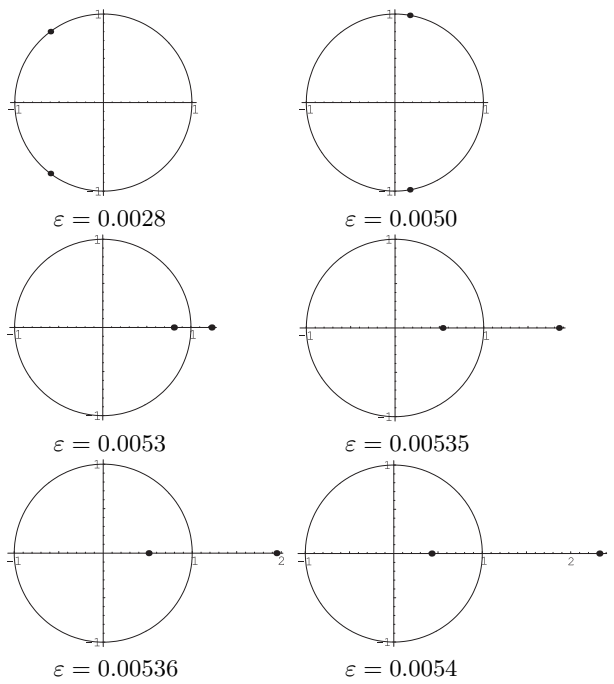

FIG. 5: The linear stability of the period-8 orbit in the $k = 3$ oscillator chain.

and compute the stability map of the central oscillator. The resulting map is presented in fig.6.

We focus to the island associated to the period-8 periodic orbit and compute the stability maps for various increasing values of the coupling parameter ε (see Fig.7). At $\varepsilon = 0.00239$ we observe that the center of the island is filled by chaotic orbits. Such chaotic region is hardly visible also for $\varepsilon = 0.00238$, where the linear stability analysis indicates the formation of complex instability (see Fig.8), which occurs and is followed by the occurrence of chaotic motion in the center of the island. By increasing the parameter ε the size of the chaotic region increases and for $\varepsilon > 0.00245$ the island disappears.

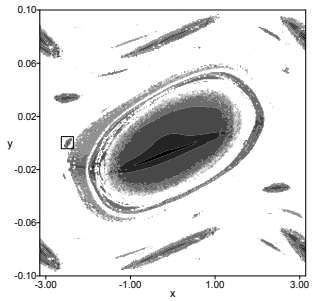

FIG. 6: Stability map for the $k = 5$ chain, using as initial conditions for the non central oscillators those obtained for the corresponding period-8 orbit.

C. Chain consisting of $k = 9$ oscillators

The nine-oscillator chain is of 7 degrees of freedom. We perform the same analysis with that for $k = 5$. There are now 14 eigenvalues of the linearized system and all of them lie on the unit circle for $\varepsilon < 0.00214$. For $\varepsilon_{cr} \simeq 0.00214$ complex instability occurs and the stability maps show chaos in the center of the island indicating in this way the instability of the periodic orbit. Fig.9 presents the passage from stability to instability.

D. Larger chains and stability

We have applied the same procedure as above in chains consisting of more oscillators and we have constructed the diagram of the number of oscillators versus the critical value of $\varepsilon = \varepsilon_{cr}$ for which the bifurcation happens and instability occurs (fig.10). For short chains ($k < 10$), we observe that ε_{cr} decrease rapidly with the size of the chain. However it seems that for larger chains ($k > 10$) the number of the oscillators does not affect the stability of a potential breather. Therefore we may conjecture that determining a stable breather for a chain of size $k \simeq 10$ this breather will still be stable in a larger chain of oscillators.

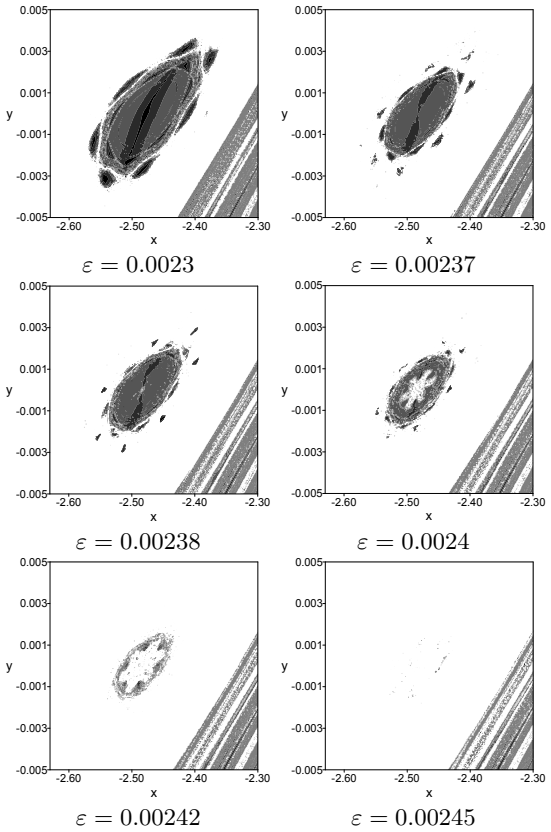

FIG. 7: The evolution of a period-8 stability island in a $k = 5$ chain for increasing values of ε.

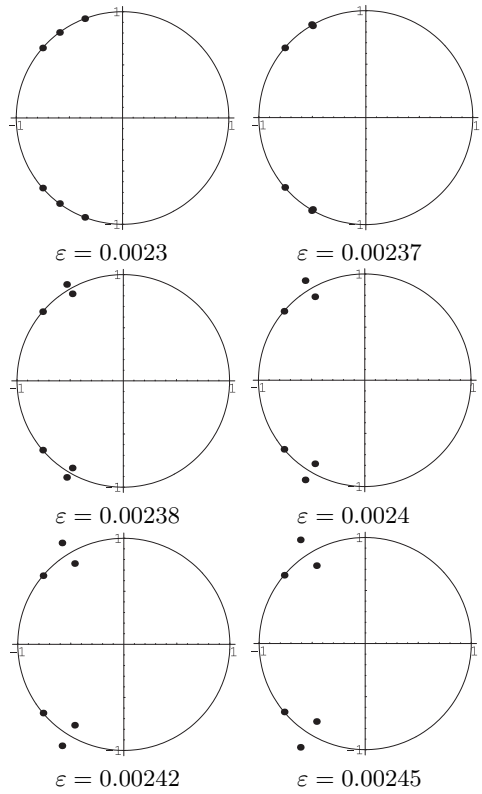

FIG. 8: The linear stability of the period-8 orbit in the $k = 5$ oscillator chain.

E. Illustration of the time evolution of DBs

Consider the time evolution of a breather solution, using as initial conditions the ones that were calculated for the $k = 31$ oscillator chain. We illustrate this evolution in fig.11. We consider two ways of representation of the breather. In fig.11a the time evolution of the x-variable of all the oscillators of the chain is shown. Note that, since we deal with discrete time, the evolution of x is considered with respect to the number of iterations n of the mapping (4). In addition, due to the discreteness of time the oscillation of x is not as smooth as it would be if we have considered continuous time t. But, showing only the x-variable is not a proper consideration since the (x, y) pair of variables is an "independent" pair and not the conjugate pair (x, p) we have when we consider Hamiltonian oscillators. So, we seek a function of x and y which will describe properly the oscillation. We, choose the value of function $F = 1.33 - \Phi$, where $\Phi = \Phi(x, y)$ is the integral of the individual oscillator , For $\varepsilon = 0$ this integral is a function of the action J only, which is directly related to the amplitude of the oscillation. The constant in F is introduced in order to have $F(0, 0) = 0$. We consider samples of the evolution of F every a multiple of q steps, where q is the period of the specific orbit (in our case $q = 8$). In this way, we obtain a measure of the variation of the amplitude of the oscillation with respect to the iterations of the map (fig.11b). In fig.11 we have the picture of a stable DB for $\varepsilon = 0.0021$. If we increase the value of ε to $\varepsilon = 0.003 > \varepsilon_{cr}$ the DB is destroyed as it was expected from the previous stability analysis (fig.12). Here we have considered samples every 32 iterations for F in order to represent a larger time period and a better dynamical picture of the destruction of the period-8 breather. This way we can see a satisfactory portion of the destruction scenario of the period-8 breather. Note that the size of the island determines also the stability region i.e.if we choose an initial condition inside the island, which is shown in fig.9 for example, the motion remains localized as it can be shown in fig.13. The variation in x is not as regular as in fig.11a, since we are not lying exactly on the periodic orbit. Also, we observe a small variation in the value of F.

IV. THE USE OF STABILITY MAPS IN LOCATING DISCRETE BREATHERS

In this section we examine if the stability maps can be used in order to locate initial conditions for discrete breathers. Since DBs are periodic orbits of the full system, the first consideration would be to locate them

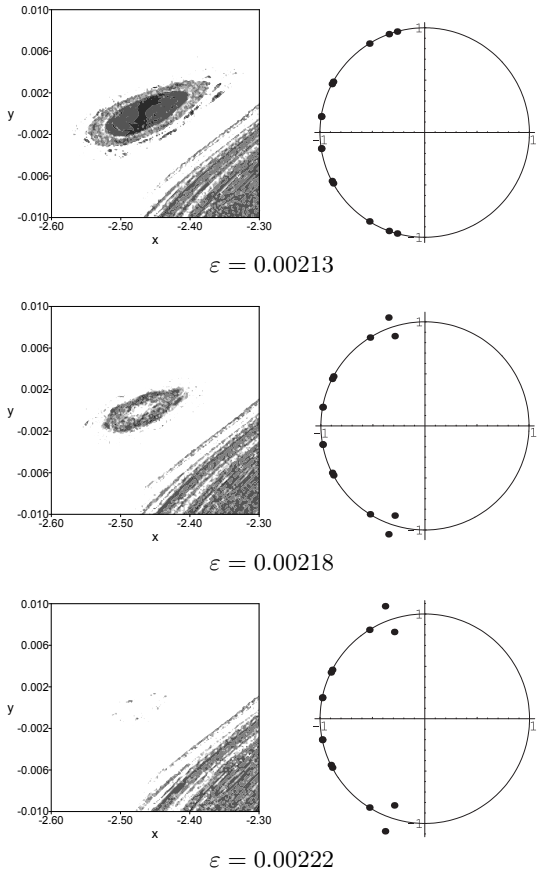

FIG. 9: The evolution of a period-8 stability island for increasing values of ε in a $k = 9$ chain (left) and the corresponding linear stability analysis (right).

through the corresponding phase space. But the system under consideration is multidimensional and thus, it is impossible to construct an illustrative phase portrait which would point out where the desired periodic orbits are located. However, since the central oscillator moves with the largest amplitude, its $x-y$ map of stability carries out the most significant information for the dynamics of the full system.

In the previous section we used as initial conditions for the oscillators (except the central one) the exact initial conditions of the periodic solution. Now we assume that such initial conditions are not known and we compute the stability map by setting all oscillators (except the central one) at rest $(x, y) = (0, 0)$.

A. The location of the period-8 Discrete Breather

For a chain consisting of $k = 5$ oscillators the stability map is given in fig.14. Now the stability islands are not well formed as in the case of fig.6 where the initial conditions of the exact periodic orbits were used. Since we are looking for the period-8 orbit, we test various small

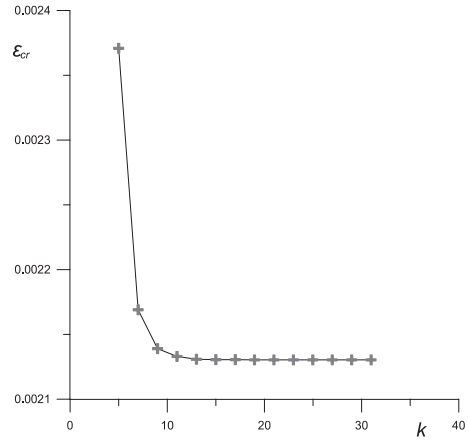

FIG. 10: The value ε_{cr} vs the size k of the chain

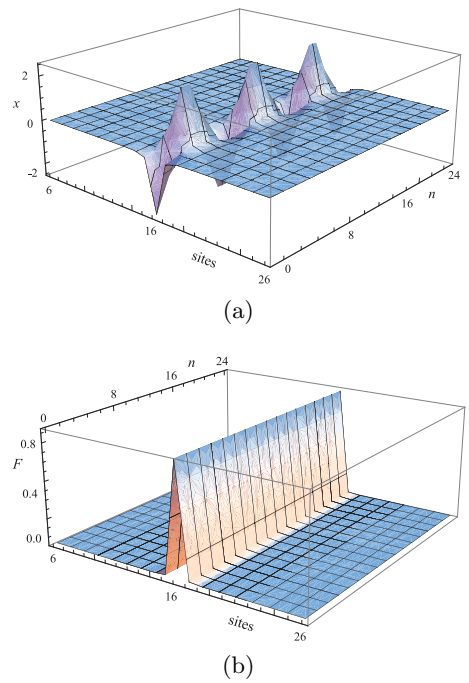

FIG. 11: The time evolution of a period-8 breather for $\varepsilon = 0.0021$. In (a) the variation of x is shown while in (b) we consider the value of F by considering samples every 8 steps.

values of the coupling parameter ε in order to observe in the stability map the corresponding stability island with sufficient clarity. In the map of fig.14 the requested chain of islands is located. By taking a magnification of the region of one of the specific islands we examine its robustness by increasing ε (Fig.15). We observe that the island disappears for $\varepsilon \simeq 0.0023$ which is close to the critical value $\varepsilon_{cr} = 0.00238$ observed in section III B. This difference is expected since in the maps of Fig.15 the oscillators, except the central one, are set initially in rest and not at the actual initial conditions of the periodic orbit and, subsequently, we lie further from the periodic

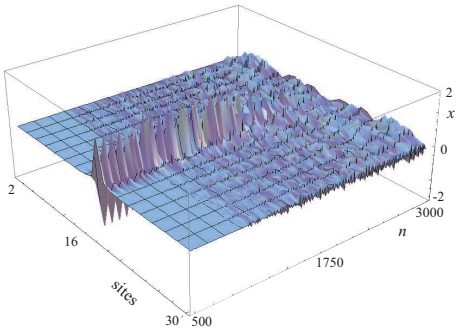

(a)

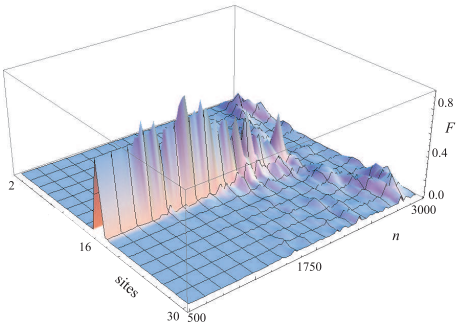

(b)

FIG. 12: The destruction of a period-8 breather for $\varepsilon = 0.003$. The representation is the same as the one in fig.11 except that we consider samples for F every 32 iterations.

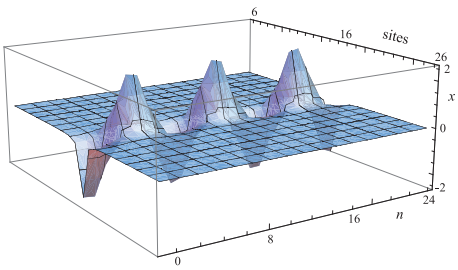

(a)

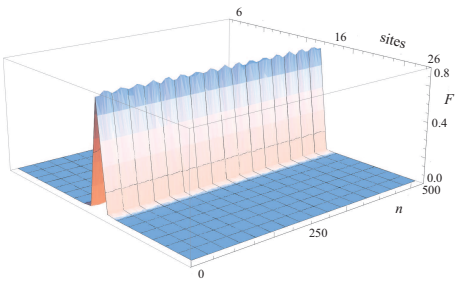

(b)

FIG. 13: The time evolution of a perturbed period-8 breather for $\varepsilon = 0.0021$. The representation is the same as the one in fig.11.

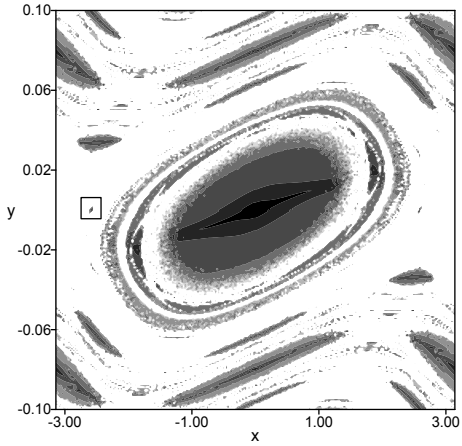

FIG. 14: A stability map of the system having initially the non-central oscillators at rest $(x, y) = (0, 0)$.

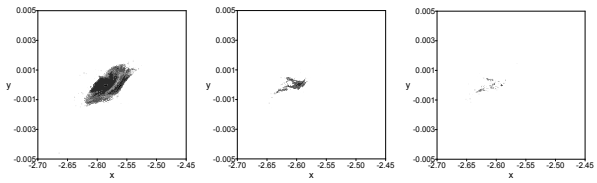

$\varepsilon = 0.00223$ $\varepsilon = 0.00233$ $\varepsilon = 0.00234$

FIG. 15: The destruction scenario of a period-8 stability island in a $k = 5$ oscillator chain

orbit than before.

If we increase the size of the system to a $k = 9$ chain, which is a critical value regarding stability for longer chains, the period-8 chain of islands is can be still located by the stability map. A magnification around a period-8 island and its evolution with respect to increasing ε is given in figures 16. The island breaks in two parts for $\varepsilon \simeq 0.00197$. The part that survives longer finally disappears for $\varepsilon > 0.00210$, close to the value $\varepsilon_{cr} = 0.00216$ in which the real periodic orbit destabilizes. For $\varepsilon < 0.002$ we can consider some initial conditions in the center (x, y) of the island for the central oscillator and (0,0) for the other oscillators in a $k = 31$ length chain, as initial estimation in a Newton-Raphson differential correction procedure, which converges and the corresponding periodic orbit is found accurately. The result is the DB that has been already shown in Fig. 11.

Another approach is the following. We can choose initial conditions inside the above mentioned island for the central oscillator e.g. $(x, y) = (-2.56, 0)$ and put the other oscillators at rest $(x, y) = (0, 0)$. Since the particular orbit is near periodic, it corresponds to a breather-like motion, which remains localized as it is shown in fig.17. In both cases (shown in figs. 13 and 17) we have not determined any difference in the time periods for which these solutions remain localized.

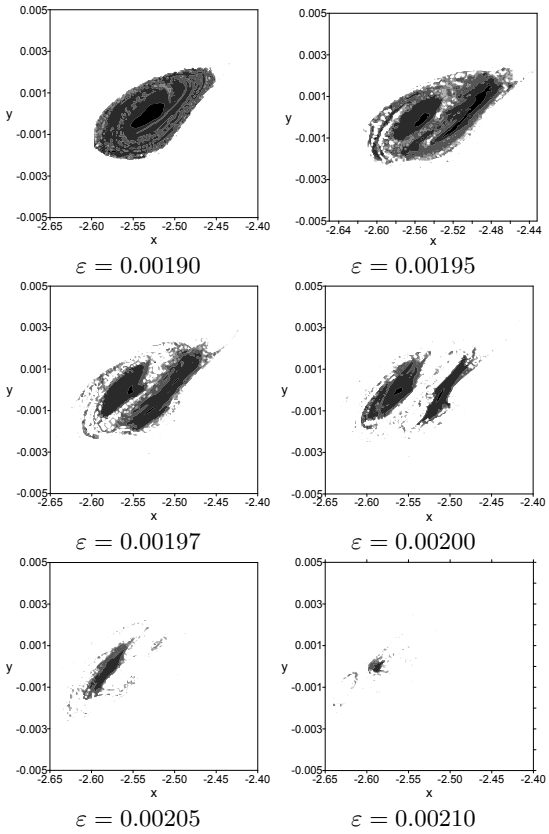

FIG. 16: The evolution of a period-8 island of stability for increasing values of ε for a $k = 9$ chain.

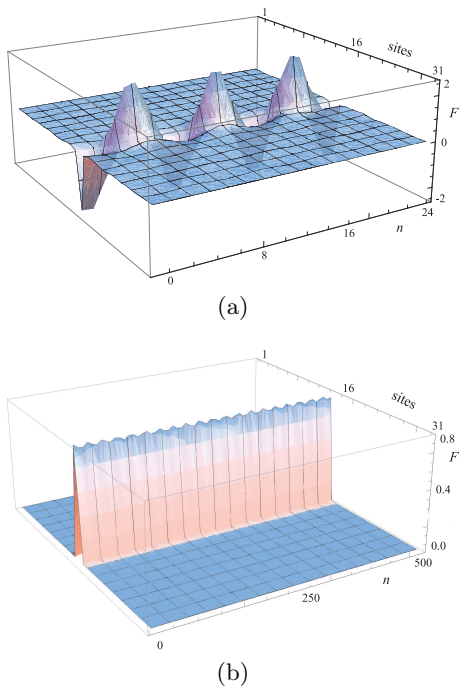

FIG. 17: The time evolution of a breather-like motion for $\varepsilon = 0.002$, which corresponds to the period-8 breather. The representation is the same as the one in fig.11.

B. A period-10 Discrete Breather

We want to show now the generality and the efficiency of the above approach. Actually we examine if we can locate other, than the period-8, DBs. According to the method described previously, we compute a stability map of initial conditions of the central oscillator having the others at rest in a $k = 9$ chain and for $\varepsilon = 0.001$. The resulting map is shown in fig.18a. We can distinguish the period-10 chain and we perform a magnification around one of the corresponding islands (fig.18b). We use one of the initial conditions inside the stability island as an initial estimation. We observe that the differential corrections converges and the periodic orbit is found. The corresponding DB is shown in fig.19.

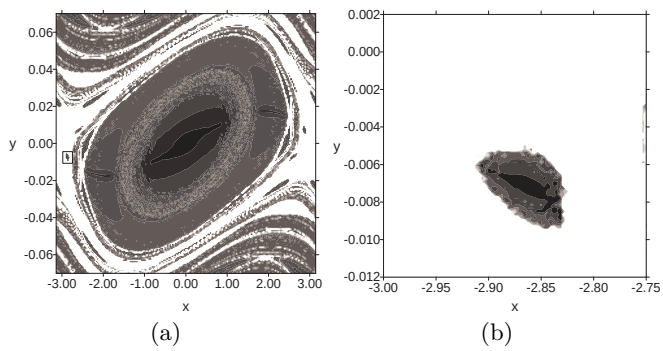

FIG. 18: The stability map for $\varepsilon = 0.001$ and $k = 9$ and a zoom around an island of the period 10 chain.

V. CONCLUSIONS

In this paper we studied the dynamics of a chain of weakly coupled symplectic mappings using stability maps. The stability maps can depict the phase space structure, namely the distribution of chaos and order, even for systems of many dimensions. Our stability maps were based on the computation of the fast Lyapunov indicator (FLI) which is a reliable and fast method for classifying the orbits as regular or chaotic even for a system of many degrees of freedom. Our study was mainly focused on periodic solutions which, for large chains, can be interpreted as spatially localized oscillations i.e. discrete breathers. The stability of such solutions were studied by using the linear analysis or by constructing appropriate stability maps.

The stability of the system has been studied as a function of the number of oscillators and as a function of the coupling parameter. Considering a system of k oscillators and a coupling parameter ε, we found that if a periodic solution is stable up to $k \simeq 10$ and for $\varepsilon < \varepsilon_{cr}$ then is stable and consist a breather for $k >> 10$ and for $\varepsilon < \varepsilon_{cr}$.

Our analysis showed that we can use the method of stability maps in order to locate initial conditions for

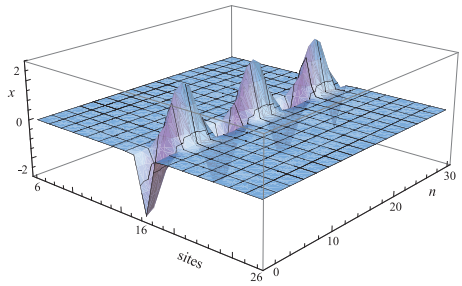

(a)

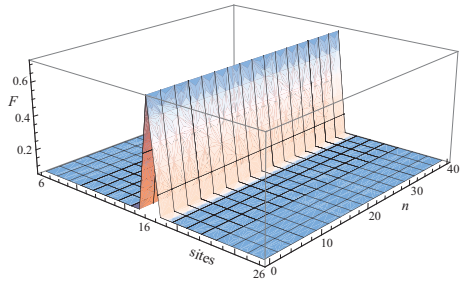

(b)

FIG. 19: The evolution of a period-10 DB for $\varepsilon = 0.001$. The representation is the same as the one in fig.11 but the samples in (b) are considered every 10 steps.

breathers. According to our framework we can detect islands in phase space by constructing stability maps. If these islands are still present and detectable up to a size of chain $k \simeq 10$ then we can use them as a first estimation in computing accurately the corresponding periodic orbit, which consist a stable breather for a large chain of oscillators. If we use directly the initial conditions of the central oscillator determined by the stability map and set the rest to $(0, 0)$ we obtain a stable but not exactly periodic oscillation (breather-like motion).

Acknowledgments. We dedicate this work to the memory of our teacher Simos Ichtiaroglou who had always been supportive and inspirational to all of us. This work has been supported by the research program "Pythagoras II' (contract No.80831) of the Greek Ministry of Education and European Union.

[1] S. Takeno, K. Kishoda, and A. Sievers, Prog. Theor. Phys. Suppl **94**, 242 (1988).
[2] R. S. MacKay and S. Aubry, Nonlinearity **7**, 1623 (1994).
[3] S. Aubry, Physica D **103**, 201 (1997).
[4] S. Flach and C. Willis, Physics Reports **295**, 181 (1998).
[5] R. S. MacKay, Physica A **288**, 174 (2000).
[6] V. Koukouloyannis and S. Ichtiaroglou, Chaos, Solitons and Fractals **13**, 1317 (2002).
[7] M. Abel and M. Spicci, Physica D **119**, 22 (1998).
[8] Y. B. Suris, Func. Anal. Appl. **23**, 74 (1989).
[9] J. Howard and R. MacKay, Journal of Mathematical Physics **28**, 1036 (1987).
[10] V. A. Yacubovich and V. M. Starzhinskii, *Linear Differential Equations with Periodic Coefficients* (Wiley, New York, 1975).
[11] V. Arnold and A. Avez, *Ergodic Problems of Classical Mechanics* (W.A. Benjamin, inc., NewYork, Amsterdam, 1968).
[12] C. Froeschlé, E. Lega, and R. Gonczi, Cel. Mech. and Dyn. Astr. **67**, 41 (1997).
[13] C. Froeschlé and E. Lega, Cel. Mech. and Dyn. Astr. **78**, 167 (2000).
[14] C. Skokos, J. Phys. A: Math. Gen. **34**, 10029 (2001).
[15] Z. Sándor, A. S. B. Érdi, and B. Funk, Cel. Mech. and Dyn. Astr. **34**, 10029 (2001).